Direct translation of incoming retroviral genomes

Julia Köppke[1], Luise-Elektra Keller[1,2], Michelle Stuck[1,3], Nicolas D. Arnow[1], Norbert Bannert[1], Joerg Doellinger[4], and Oya Cingöz[1,*]

[1] Robert Koch Institute, Department of Infectious Diseases, Unit of Sexually Transmitted Bacterial Pathogens and HIV (FG18), Berlin, Germany

[2] Current address: Institute of Cardiovascular Regeneration, Goethe University Frankfurt, Germany

[3] Current address: Department of Chemistry, Heidelberg University, Heidelberg, Germany

[4] Robert Koch Institute, Center for Biological Threats and Special Pathogens, Proteomics and Spectroscopy (ZBS6), Berlin, Germany

* To whom correspondence should be addressed. Email: cingoezo@rki.de

Abstract

Viruses that carry a positive-sense, single-stranded (+ssRNA) RNA translate their genomes soon after entering the host cell to produce viral proteins, with the exception of retroviruses. A distinguishing feature of retroviruses is reverse transcription, where the +ssRNA genome serves as a template to synthesize a double-stranded DNA copy that subsequently integrates into the host genome. As retroviral RNAs are produced by the host cell transcriptional machinery and are largely indistinguishable from cellular mRNAs, we investigated the potential of incoming retroviral genomes to directly express proteins. Here we show through multiple, complementary methods that retroviral genomes are translated after entry. Our findings challenge the notion that retroviruses require reverse transcription to produce viral proteins. Synthesis of retroviral proteins in the absence of productive infection has significant implications for basic retrovirology, immune responses and gene therapy applications.

Introduction

All viruses, regardless of their nucleic acid type, composition or orientation, need to reach the mRNA stage for successful infection. Retroviruses carry two copies of a positive-sense, single-stranded RNA (+ssRNA) genome; however, they form a separate class from +ssRNA viruses in the Baltimore classification because their replication strategy involves reverse transcription of the ssRNA genome into a double-stranded (dsDNA) copy. Based on current knowledge most if not all +ssRNA viruses directly translate their RNA to synthesize viral proteins upon entry into host cells, with the exception of retroviruses, which undergo reverse transcription and degrade the original genomic RNA in the process. As retroviral genomes are produced by the host cell machinery, with a 5' cap and a 3' poly-A tail, we asked: Are incoming retroviral genomic RNAs also directly translated?

One small but notable difference between the full-length retroviral RNA packaged into the virions as the genome and the one that produces Gag and GagPol polyproteins is their transcription start sites (TSS). Full-length retroviral RNAs contain heterogenous TSS, which alters the RNA structure and impacts its dimerization and translation potential.[1, 2, 3] While 1G transcripts are primarily dimerized and selectively packaged into virions, 2G and 3G transcripts exist mainly as monomers and are enriched in polysomes.[1, 2] In addition, incompletely-spliced retroviral transcripts carry hypermethylated caps bound by NCBP3 instead of eIF4E, and translated in an mTOR-independent manner, although such hypermethylated caps were not detected in virion-packaged RNA.[4] As genomic RNA isolated from virions can be translated in *in vitro* systems to produce retroviral proteins,[5, 6, 7] the virion-packaged genomic RNA does not appear to be inherently untranslatable, even if it differs from the newly-produced full-length RNA that is translated to produce viral structural proteins.

Using multiple complementary approaches, including post-translational regulation of protein stability coupled to sensitive reporter assays, immunoprecipitation, polysome fractionation and SILAC-based mass spectrometry, we demonstrate here that incoming retroviral RNA genomes are translated shortly after cellular entry. This is a general process that occurs under a variety of conditions; with different viral genome lengths, cellular entry pathways and cell types. Extensive controls including nuclease treatments, checking for DNA or protein transfer, using fusion-defective viruses, and omission of various viral components (e.g. *env*, *gag*, packaging signal) confirm that the signal is truly due to direct *de novo* translation from incoming genomes. Capsid mutants that display altered stability and uncoating kinetics impact the translation of incoming RNAs by regulating the access of the encapsidated RNA to the translational machinery. The synthesis of retroviral proteins in the absence of reverse transcription has significant implications for basic retrovirology, immune responses during infection, and the use of retroviral vectors as RNA delivery vehicles.

47 # Results

48 **Post-translational control of protein stability minimizes virion-packaging and cellular delivery of**
49 **reporter proteins**

50 In the laboratory, retroviruses are typically produced by transfection of producer cells with
51 plasmids encoding viral components. In case of viral genomes that carry a reporter gene, the reporter
52 protein is also expressed in producer cells, which can get packaged into virions and delivered into
53 recipient cells, yielding false positives.[8, 9, 10, 11, 12, 13] To minimize such producer cell background, which
54 could mask the signal from *de novo* translated incoming retroviral RNAs, we employed a post-
55 translational protein control system (ProteoTuner), where a destabilizing domain (DD) derived from a
56 cellular gene with a very short half-life (FKBP12) is fused to the gene of interest, targeting it for rapid
57 proteasomal degradation.[14] The unstable protein can be stabilized in a dose-dependent and
58 reversible manner by adding a cell-permeable small molecule ligand called Shield1 that binds to the
59 DD, allowing post-translational regulation of protein levels. We reasoned that producing viruses in
60 the absence of the ligand would minimize reporter protein packaging into virions, whereas
61 performing infections in the presence of the ligand would allow us to detect reporter expression
62 from the incoming retroviral RNA genomes by stabilizing the reporter. As only two genomic RNAs per
63 retrovirus particle are delivered into the cell upon entry, we selected the sensitive reporter nano-
64 luciferase (Nluc) to assay the translation of incoming retroviral RNA genomes, which has superior
65 sensitivity compared to other luciferase proteins (reviewed in [15]).

66 Nluc was cloned with or without the DD either under a CMV promoter in a minimal lentiviral
67 vector to produce pLVX-(DD)-Nluc, or with deletions in the CMV promoter, IRES element and Neo
68 resistance gene to generate pLVX-(DD)-Nluc-ΔCIN (Fig. 1A). Transfection of these constructs into
69 293T cells resulted in 30-45-fold less luciferase activity in case of DD-harboring constructs, while
70 Shield1 treatment rescued the expression (Fig. 1B). The stabilization of DD-Nluc constructs by Shield1
71 was dose-dependent, whereas Nluc constructs without the responsive domain remained unaffected
72 (Fig. 1C). To quantify the amount of reporter protein packaging into virions, we produced virions by
73 transfecting cells with the lentiviral transfer vectors shown in Fig. 1A along with a packaging
74 construct with or without an *env* plasmid (VSV-G) and assayed the virus particles themselves for
75 luciferase activity. Virions produced by DD-Nluc vectors consistently yielded 120-270-fold lower
76 signal compared to Nluc vectors for both constructs, while the presence or absence of an envelope
77 protein (VSV-G) did not make a difference (Fig. 1D).

78 For HIV-1, the timing of the early events during infection are well-documented and cell type-
79 dependent. Reverse transcription can take anywhere from 6 - 48 hours, and integration follows about
80 5 hours after the completion of reverse transcription.[16, 17] As the constructs in Fig. 1A cannot produce
81 the reporter protein from full-length (unspliced) viral RNA, they require reverse transcription,
82 integration, transcription, splicing and translation to express luciferase. Accordingly, within the first
83 12 hours of infection, no change in signal was observed, indicating that the luciferase signal
84 represents Nluc protein that is transferred to and/or that remains associated with cells (Fig. 1E). The
85 presence or absence of an Env protein or the RT inhibitor nevirapine (NVP) had no effect on the
86 signal observed, although infection with the destabilized reporter viruses consistently yielded less
87 signal. Likewise, at 20 hours post-infection, there is still no expression from the provirus, but
88 expression did occur at 72 hours post-infection (hpi), which was reduced to background levels in the
89 absence of a functional Env or reverse transcription (Fig. 1F). These data show that post-translational
90 regulation of protein stability can markedly reduce passive protein packaging into virions and their
91 delivery into recipient cells, minimizing the background for assessment of incoming retroviral RNA
92 translation.

93 **Incoming retroviral genomes are used as an mRNA for protein expression early after entry**

94 To assess the direct translation potential of the full-length, incoming retroviral genomic RNA,
95 we cloned Nluc with or without the DD downstream of the packaging signal (Ψ; psi) in place of where
96 *gag* would normally be in a minimal lentiviral vector. The start codon of *gag* was mutated and any
97 additional elements that could affect translation efficiency (e.g. IRES, WPRE) were removed (Fig. 2A).
98 In line with previous results, transfection of DD-constructs resulted in ~180-fold decreased signal
99 compared to Nluc, which was completely rescued by Shield1 (S1) addition (Fig. 2B). We produced
100 virions and infected cells with serial dilutions of LV-DD-Nluc virus in the presence of NVP and S1, with
101 or without the translation inhibitor cycloheximide (CHX) to distinguish virion-packaged protein
102 delivery from *de novo* translation. Using viral doses as low as 0.0061 ng p24 per 100K cells, we
103 detected a CHX-sensitive signal (Fig. 2C). The signal to noise ratio (i.e. new protein synthesis vs.
104 packaged protein delivery) was highest between 0.165-4.5 ng p24 per 100K cells. Based on these
105 results, we opted to use 1-4 ng p24 in subsequent experiments.

106 Infection of cells with LV-Nluc virus resulted in an increase in the luciferase signal over time
107 despite the background of virion-packaged protein, which was diminished to background levels by
108 CHX treatment (Fig. 2D). RT inhibition had no effect on the luciferase signal within the first 8 hours,
109 indicating that the translation occurs independently of reverse transcription. We then performed an
110 infection with LV-DD-Nluc virus in the presence of NVP. The signal increased within the first 2 h, and

111 under S1-stabilized conditions increased further up to 6 h, whereas in the absence of S1, it decreased
112 after the initial hike due to the instability of the protein (Fig. 2E; red vs. blue lines). Translation
113 inhibition by CHX drastically reduced the signal in both cases, although increased stabilization of the
114 protein delivered passively by virions was also evident (Fig. 2E; green vs violet lines). Importantly,
115 when DD-Nluc is stabilized, there is a clear increase in reporter expression over time, which is
116 markedly reduced upon translation inhibition (Fig. 2E; red vs. violet lines). This difference is the result
117 of newly synthesized reporter proteins from the incoming retroviral genomic RNA in the absence of
118 reverse transcription. Similar results were observed regardless of whether the initial inoculum was
119 kept on the cells or whether the virus was removed after one hour, although the lack in continuous
120 virus uptake in the latter case was evident (Fig. 2F-G).

121 **Expression from incoming retroviral genomes is due to *de novo* translation and occurs under**
122 **different conditions**

123 Viral supernatants typically contain plasmids carried over from transfected producer cells.
124 Pre-treatment of our virus stocks with nucleases that degrade either DNA, RNA or both did not alter
125 reporter expression from the incoming viral genome after transduction, despite the enzymes being
126 functional, indicating that the observed signal is not due to nonspecific uptake of ambient DNA or
127 RNA (Fig. 3A-B). The presence of a functional viral envelope on particles was necessary, as viruses
128 pseudotyped with a VSV-G mutant defective in fusion activity (P127D) or those without an Env failed
129 to yield a signal above background (Fig. 3C). Similar results were observed with Gag-less "virus"
130 supernatants, when the packaging plasmid was omitted during virus production (Fig. 3D). To ensure
131 that our observations are not due to incomplete inhibition of RT, we confirmed these results with
132 viruses containing a catalytic mutant RT (Fig. 3E and Supp. Fig. 1A). To rule out endogenous reverse
133 transcripts already present in virions or the inadvertent packaging and delivery of plasmid DNA
134 fragments from producer cells as the source of the reporter signal, neither of which would be
135 susceptible to nuclease digestion, we transduced cells in the presence of transcription or translation
136 inhibitors (Actinomycin D [ActD] or CHX, respectively). Translation inhibition markedly reduced the
137 signal as shown previously (Fig. 2C-G), whereas transcription inhibition did not, indicating that the
138 observed signal is not due to DNA transfer, which would have required both of these processes (Fig.
139 3F). At the same concentrations both drugs inhibited expression from a transfected reporter plasmid,
140 validating their functionality (Fig. 3G). Although inhibition of reverse transcription is not required for
141 this process, we also confirmed these results during transduction in the presence of different RT
142 inhibitors, namely NVP, efavirenz (EFV) and tenofovir (TAF) used at 10 µM (Fig. 3H), which resulted in
143 similar expression levels as the untreated sample. When these RT inhibitors were used at higher
144 concentrations (100 µM) during infection, toxicity to cells was evident particularly in case of EFV,

145 where cells also lost the ability to express a transfected plasmid (Supp. Fig. 1B-C). Notably, the
146 translation of incoming retroviral genomes was observed with viral envelopes that use different entry
147 pathways (Fig. 3I) and in diverse cell lines and primary cells (Fig. 3J), indicating that this is a broad
148 process not restricted to a specific cell type or condition.

149 **Immunoprecipitation, SILAC/MS and polysome fractionation confirm direct expression from**
150 **incoming HIV-1 genomes**

151 The RNA genome of HIV-1 has an intricate secondary structure and several *cis*-acting RNA
152 elements with diverse functions in the replication cycle, which are not all present in the context of a
153 minimal vector.[18] To explore the contribution of such RNA elements to the process of incoming
154 retroviral genomic translation, we cloned DD-Nluc downstream of the packaging signal and a
155 mutated *gag* start codon in a near-full length HIV-1 construct based on NL4.3 that encodes firefly
156 luciferase in place of *nef* (Fig. 4A). Infection with NL43-DD-Nluc, produced by co-transfecting cells
157 with a packaging plasmid and a VSV-G *env*, yielded similar results to infection with minimal lentiviral
158 vectors in the presence of NVP (Fig. 4B vs. Fig 2E & 2G). Under S1-stabilized conditions the signal
159 increased over time, peaking at 4-6 hpi, whereas translation inhibition reduced the reporter activity
160 to baseline levels, confirming *de novo* protein synthesis (Fig. 4B; red vs. violet lines). Based on the
161 relatively short incubation times, we did not remove the virus inoculum, which explains why the
162 stabilized CHX condition shows a slight increase over time due to continuous reentry (violet line).

163 To evaluate the number of RNA copies delivered into cells, we performed transductions with
164 the parental NL43-Firefly virus in the presence or absence of NVP and quantified post-entry events at
165 24 and 48 hours. As infection with 4 ng p24 per 100K cells did not yield a detectable signal for RT
166 products above background, we performed infections using 10 times more virus than normally used,
167 which corresponds to a multiplicity of infection (MOI) of 1 based on the transducing units validated
168 by p24 staining. Under these conditions, we detected early RT products between 4.1 - 8.2 copies, late
169 RT products between 2.4 - 4.1 copies, and 2-LTR circles between 0.02 - 0.03 copies per haploid
170 genome (Supp. Fig. 2A).

171 As an alternative to reporter assays, we checked Gag protein production in the absence of
172 reverse transcription. Cells were challenged with VSV-G-pseudotyped NL43-Firefly virus (MOI = 1) in
173 the presence or absence of NVP and CHX. Gag production was assayed by immunoprecipitation (IP)
174 with an anti-Gag polyclonal antibody and western blot one day after infection to maximize the
175 accumulation of newly-synthesized viral proteins. In the absence of RT inhibition, Pr55-Gag was
176 produced at this time point, as expected. Although NVP treatment decreased this signal, viral protein

177 production was still evident and did not originate from incoming CA protein, as CHX treatment
178 abolished this signal (Fig. 4C).
179 To provide further evidence that authentic viral proteins are produced from the packaged
180 viral genome, we performed metabolic labeling via stable isotope labeling with amino acids in cell
181 culture followed by mass spectrometry (SILAC-MS). Briefly, cells grown in light medium were
182 transduced with VSV-G-pseudotyped NL43-Firefly virus also produced in light medium (MOI = 0.5). At
183 the time of transduction, cells were switched to heavy medium such that all newly produced proteins
184 would be heavy, whereas all pre-existing proteins light. After 18 hours, lysates were subjected to
185 immunoprecipitation with an anti-p24 antibody followed by mass spectrometry. Under conditions
186 where reverse transcription could take place, *de novo* viral Gag production was evident, as cells had
187 enough time to undergo the regular replication steps (Fig. 4D). Importantly, although the ratio of
188 heavy to light peptides that map to Gag were lower in case of RT inhibition, such peptides were still
189 detected, validating that incoming HIV-1 genomes are translated to produce viral proteins. Heavy
190 peptides corresponding to Gag were only detected under conditions where translation could take
191 place, confirming that these results truly are the result of *de novo* translation (Fig. 4D).

192 To validate the association of incoming HIV-1 RNA with polysomes - an indicator of active
193 translation - we also performed polysome fractionation on lysates from 293T cells after four hours of
194 infection with VSV-G-pseudotyped IIIB with a catalytic RT mutation (DD185/186AA; Supp. Fig. 1A).
195 Infected and uninfected cells yielded comparable polysome profiles with clearly separated peaks for
196 ribosomal subunits, whereas EDTA treatment completely disrupted polysomes (Fig. 4E). RT-qPCR on
197 fractions demonstrated the association of 10% and 72% of all HIV-1 RNA and the housekeeping gene
198 *HPRT1* (hypoxanthine phosphoribosyltransferase-1 RNA) with polysomes, which was reduced to 1%
199 and 2% in EDTA-treated controls, respectively, indicating specific association of these RNAs with
200 polysomes (Fig. 4F). Taken together, these data provide multiple independent lines of evidence that
201 demonstrate the production viral proteins in the absence of reverse transcription.

202 **Packaging signal and capsid stability mutations impact the course of incoming retroviral RNA**
203 **translation**

204 The packaging signal (Ψ; psi) found in retroviral genomes is critical for the selective packaging
205 of the full-length viral RNA into budding virions (reviewed in [19]). Deletion of 38 nucleotides (750-787)
206 downstream of the Gag start codon in LV-DD-Nluc (ΔΨ) drastically reduced the amount of packaged
207 genomic viral RNA compared to WT (Fig. 5A), even though the expression from the ΔΨ construct by
208 transfection was comparable to WT with a 2.5-fold increase (Fig. 5B). Infection of cells with the two
209 viruses showed significantly reduced reporter signal in ΔΨ compared to WT, indicating that the

210 packaging of the viral genome into particles is essential for incoming viral RNA translation, as
211 expected (Fig. 5C).

212 Since the viral RNA genome is protected by the capsid, we reasoned that mutations affecting
213 capsid stability may alter incoming translation kinetics. To this end, we used two well-characterized
214 capsid mutants; the hypostable P38A mutant that loses its integrity early after entry, and the
215 hyperstable E45A mutant which does not easily dissociate. It was previously described that different
216 titration methods show considerable variation in predicting the transducing units of lentiviruses.[20]
217 We therefore normalized the viruses to each other by different methods: p24-CA amount by ELISA,
218 viral genomic RNA by RT-qPCR, virion-packaged Nluc by luciferase assay, or simply by using equal
219 volumes from viruses produced at the same time. Despite slight variations based on the
220 normalization method used (Fig 5D-E and Supp. Fig. 3A-B), collectively, infection with the P38A
221 mutant increased translation from incoming genomes compared to WT, whereas E45A mutant
222 decreased it (Fig. 5F). These data are consistent with unstable capsids allowing increased access to
223 the translational machinery, in contrast to hyperstable capsids shielding the viral RNA, linking capsid
224 stability and uncoating kinetics to the translation potential of incoming retroviral genomes.

225 We show here that the RNA genome packaged into retroviral particles can serve as an mRNA
226 for viral protein production independently of reverse transcription. This process occurs in the context
227 of both minimal and near full-length genomes, in the presence of RT inhibitors and catalytic mutants,
228 with Env proteins that use different entry pathways and in different cell types with different virus
229 amounts, suggesting that this is a general process. Using thorough controls that account for nucleic
230 acid contamination, passive DNA or protein delivery, transcription and translation inhibitors, fusion-
231 deficient envelopes and omission of various viral components, we confirm that the signal observed is
232 due to *de novo* translation. Using capsid mutant viruses, we further demonstrate that the translation
233 potential of the viral RNA is linked to capsid stability as the process of uncoating modulates the
234 access of the incoming RNA to ribosomes. In summary, we provide multiple lines of evidence that the
235 retroviral genome can serve as an mRNA early after cellular entry. Below we discuss potential
236 implications of our findings for basic retrovirology, host immune responses and RNA delivery
237 approaches.

238 Discussion

239 Early studies of avian and murine retroviruses reported the detection of full-length viral
240 genomes in polysome-containing pellets within 4 hpi.[21, 22, 23] A recent study also detected full-length
241 HIV-1 transcripts associated with polysomes at 8 hpi; although it is unclear whether the expression at

242 this time point is mediated by reverse-transcribed and integrated viral DNA that is then newly-
243 transcribed, or from the incoming RNA genome itself, as the HIV-1 RT was functional in this case.[24] In
244 support of our findings, a ribosome profiling study of HIV-1 infected cells detected ribosome-
245 protected RNA fragments indicative of active translation in the *gag* coding region already within one
246 hour of infection.[25] Based on the current knowledge regarding infection kinetics, as one hour is too
247 short of a time period to complete reverse transcription and integration, the implication is that such
248 expression is enabled by the direct translation of the RNA genome. Ribosome profiling studies in the
249 absence of a functional RT at early time points following infection will be informative in identifying
250 the specific regions of incoming retroviral genomes that are translated in different cell types.
251 In the field of gene therapy, recombinant retroviral vectors are very well-characterized and
252 commonly used as tools for nucleic acid or protein delivery (reviewed in [26]). In a previous study using
253 minimal gammaretroviral (MLV) vectors with primer binding site (PBS) mutations that cannot initiate
254 reverse transcription, protein expression from a reporter gene was detected.[27] In other studies,
255 modified lentiviral vectors containing 5' IRES or 3' WPRE insertions or major structural
256 rearrangements of the genome (e.g. moving the U5-R regions further downstream towards the 3'
257 end) were employed in order to enable direct translation from the packaged RNA.[28, 29] In all of these
258 studies, however, protein or DNA transfer cannot be ruled out. In addition, to our knowledge, the
259 production of actual retroviral proteins from a (near) full-length genome in the absence of reverse
260 transcription has not been demonstrated.
261 A paradigm shift in retrovirology occurred with the finding that intact or near-intact HIV-1
262 capsids can be transported into the nucleus, where reverse transcription and uncoating is
263 completed.[30, 31, 32, 33] How to reconcile the direct translation of incoming retroviral genomes
264 surrounded by capsid and inaccessible to the translational machinery with the detection of intact
265 core structures in the nucleus? In a given virus population not all particles are infectious or
266 replication-competent. In fact, for animal viruses the particle-to-PFU (or particle to infectious unit;
267 P/IU) ratio can vary greatly; from 1-2 for Semliki Forest Virus to as high as 10^7 for HIV-1, according to
268 some estimates (reviewed in [34]). Such a high ratio highlights the presence of a large number of
269 particles that may not proceed successfully to next steps of the replication cycle. We believe that
270 incoming retroviral RNA translation occurs in case of particles that are able to enter the host cell,
271 carry a packaged genomic RNA and start uncoating before reaching the nucleus; an idea that has
272 been employed as a basis for the EURT entry/uncoating assay.[35] As direct translation of the genome
273 is likely a dead-end for viral replication, it is reasonable to assume that virions that end up producing
274 infectious progeny are the few ones that successfully make it to the nucleus or the nuclear pore
275 intact, not those that are translated. In the stochastic environment of a viral population, some

276 genomes are translated, whereas some are reverse transcribed, just as some capsids fall apart before
277 reaching the nucleus while some of them make it to the nucleus almost intact. As many of the assays
278 used in this study are biochemical in nature, we cannot analyze the status of individual virus particles
279 but rather the status of the population as a whole. Single-molecule live-imaging approaches to
280 visualize incoming viral genomic RNAs and newly-synthesized proteins will be valuable in quantifying
281 the percentage of particles that are translated after cellular entry.

282 The production of viral proteins in the absence of reverse transcription could have major
283 consequences. Individuals who encounter HIV-1 but who do not get productively-infected, for
284 instance due to pre-exposure prophylaxis (PrEP) usage, may still be able to process and present viral
285 peptides to generate cell-mediated and/or humoral immune responses. An initial abortive infection
286 may result in the recruitment and activation of T-cells, increasing the eligible target cell population
287 locally for productive infection. During SIV infection of rhesus macaques, Gag- and Pol-specific CTL
288 responses were identified very early (within 2h) after infection, whereas Env- or Nef-specific
289 responses were not found until later, which was attributed to the ability of incoming viral proteins to
290 be processed and presented.[36,37] Data presented here suggest that such responses may also occur
291 due to *de novo* translation from the viral genome. In summary, our results challenge the notion that
292 retroviruses require reverse transcription to produce viral proteins, warrant careful studies of
293 immune responses during abortive infection and open up novel avenues for gene therapy and
294 targeted vaccine approaches.

295 Methods

296 **Cloning, constructs and virus production.** As a basis for minimal lentiviral vectors the pLVX-
297 IRES-Neo vector (Clontech) was used, which contains identical, full-length LTRs. DD-Nluc was
298 synthesized as a gBlock (IDT) and cloned between XhoI and NotI sites of pLVX-IRES-Neo, either with
299 or without the destabilizing domain to create CMV-(DD)Nluc. Similarly, (DD)Nluc was cloned between
300 ClaI and MluI sites of pLVX-IRES-Neo to eliminate the CMV promoter, multiple cloning site, IRES
301 element and Neo resistance gene to create (DD)Nluc-WPRE. LV-(DD)Nluc was created first by deleting
302 the sequences between ClaI and KpnI sites (including CMV promoter, multiple cloning site, IRES
303 element, Neo resistance gene and the WPRE sequence) in pLVX-IRES-Neo and religating the vector
304 onto itself, then mutating the start codon of Gag, inserting the restriction sites BstBI and PacI after
305 the packaging signal (Ψ) and finally cloning (DD)Nluc between these restriction sites. Packaging signal
306 deletion (ΔΨ) was introduced into LV-DD-Nluc by overlap PCR resulting in a deletion between
307 nucleotides 750-787 based on the pLVX-IRES-Neo vector sequence. NL43-Firefly is pNL4-3 e- r- FLuc
308 (kindly provided by Ned Landau; NIH ARP-3418). NL43-DD-Nluc was created by mutating the Gag

309 start codon of NL43-Firefly and inserting the DD-Nluc sequence between PteI and SpeI sites. The
310 identity of all constructs was confirmed by restriction digest and sequencing.
311 Reporter viruses were produced by transfecting viral plasmids together with a plasmid
312 encoding VSV-G *env* (pCMV-VSV-G-myc, or the fusion-defective mutant P127D, kindly provided by
313 Wes Sundquist; Addgene #80054 and #80055), and in case of the minimal lentiviral vectors or NL43-
314 DD-Nluc, also with a packaging plasmid encoding HIV-1 gag, pol, tat and rev (psPAX2, kindly provided
315 by Didier Trono; Addgene #12260) or with the packaging plasmid pCD/NL-BH*deltavpu/RT- that
316 lacks RT activity due to the D110E mutation in the catalytic site (kindly provided by Jakob Reiser;
317 Addgene #136985). CA stability mutants P38A and E45A were kindly provided by Stephen Goff. The
318 full-length IIIB ΔRT construct carrying the DD185/186AA mutations in the catalytic domain of RT was
319 kindly provided by Michael Malim.[38] The HIV-1 *env* plasmid was kindly provided by Yiping Zhu
320 (University of Rochester). X-MLV *env* was a codon-optimized, V5-tagged, synthetic Xenotropic MLV-
321 Related Virus (XMRV) *env* in a pTH backbone, kindly provided by Alaa Ramadan.[39]
322 Virus stocks were produced by transfection of 293T cells with polyethylenimine (PEI),
323 followed by media change after one day and supernatant collection after two days. ΔEnv or ΔGag
324 viruses were produced by omitting the respective plasmids during the transfection step. Virus-
325 containing supernatants were filtered (0.45 µ), ultracentrifuged over a 20% sucrose cushion,
326 aliquoted and frozen at -80°C. Nuclease treatment of virus stocks was performed at room
327 temperature by DNase (Ambion), RNase (Qiagen) or benzonase (Millipore).
328 **Cell culture, treatments, transductions.** 293T and TZM-bl cells were maintained in DMEM
329 containing 9% FBS (Gibco) and 100 µg/ml Pen/Strep (Gibco). All suspension cell lines including THP-1,
330 U937, C8166, Jurkat, PM1 and A3.01 were maintained in RPMI with 9% FBS, 100 µg/ml Pen/Strep,
331 100 µg/ml Normocin (Invivogen). PBMCs of healthy donors were isolated from buffy coats from the
332 German Red Cross using standard Ficoll separation. Monocytes were selected by adhering PBMCs in
333 RPMI with 5% pooled AB human serum (Sigma), 1 mM HEPES (Gibco) and 24 µg/ml gentamicin
334 (Sigma) for several hours, followed by extensive washing to remove unbound cells. Monocyte-
335 derived macrophages were differentiated from primary monocytes by 50 ng/ml GM-CSF (R&D
336 Systems) treatment for 6-10 days. CD4+ T-cells were isolated from PBMCs by negative selection using
337 the MACS human CD4+ T-cell isolation kit (Miltenyi). Infections were performed by spinoculation at
338 1200 x g for 60-90 mins at 25°C. Unless indicated otherwise, the following concentrations were used
339 for treatments: NVP: 10-25 µM (Merck), CHX: 10-100 µg/ml (EMD/Millipore), ActD: 2 µg/ml (Sigma),
340 Shield1: 1.5-3 µM (Takara). With the exception of time-course experiments, Nluc activity was
341 measured after 4-6 hours post-infection, using the Nano-Glo luciferase assay system (Promega).

342 **Polysome fractionation.** Polysome fractionation was performed as previously with some
343 modifications.[40] Cells were split the day before such that they would reach a maximum of 60-80%
344 confluency on the day of the assay. At four hours post-infection with RT-deficient viruses or with WT
345 viruses in the presence of NVP treatment, cells were treated with 50 µg/ml CHX for 10 min at 37°C,
346 washed once with ice-cold PBS + CHX (50 µg/ml), collected by scraping in PBS+CHX, pelleted, and
347 lysed in 1X polysome lysis buffer containing 20 mM Tris-HCl pH 7.5, 150 mM KCl, 5 mM $MgCl_2$, 0.5 %
348 NP40, 1 mM DTT, 50 µg/ml cycloheximide, and protease inhibitors (Roche) on ice for 10 mins. Lysates
349 were passed through a 21-gauge needle 12 times, incubated on ice for another 5 mins and cleared by
350 spinning at 4°C, 13.000 rpm for 10 mins. Cleared lysates were then loaded on 15-45% linear sucrose
351 gradients (in 20 mM Tris-HCl pH 7.5, 150 mM KCl, 5 mM $MgCl_2$, 50 µg/ml CHX) prepared using a
352 BioComp gradient master in ultra-clear centrifuge tubes (Beckman Coulter) and centrifuged for 2:30
353 hours at 36.000 rpm in an SW41 rotor. Fractions (0.5 ml) were collected by a piston gradient
354 fractionator (Biocomp) with continuous UV absorbance recording at 254 nm. RNA from each fraction
355 was isolated by phenol-chloroform extraction and quantified by RT-qPCR.

356 **qPCR, RT-qPCR.** Viral genomic RNA was isolated from concentrated virus stocks with viral
357 RNA isolation kit (Qiagen). RNA was treated with Turbo DNase and inactivation beads (Ambion),
358 cDNA was synthesized using Superscript III (Invitrogen) or RevertAid RT (Thermo) with random
359 hexamers (Roche). qPCR was performed with the SensiFAST No-ROX Probe Master Mix (Bioline) on a
360 CFX96 qPCR machine (Bio-Rad) along with standards. Primer and probe sequences used in RT-qPCR
361 are listed in Table 1.

Target	F/R/P	Sequence	Reference
RT products	F	TGTGTGCCCGTCTGTTGTGT	41
	R	GAGTCCTGCGTCGAGAGATC	
	P	CAGTGGCGCCCGAACAGGGA	
2-LTR circles	F	AACTAGGGAACCCACTGCTTAAG	
	R	TCCACAGATCAAGGATATCTTGTC	
	P	ACACTACTTGAAGCACTCAAGGCAAGCTTT	
HIV-1 genome	F	TCTCGACGCAGGACTCG	42
	R	TACTGACGCTCTCGCACC	
	P	CTCTCTCCTTCTAGCCTC	
HPRT1 mRNA	F	TCTTTGCTGACCTGCTGGATT	
	R	TTATGTCCCCTGTTGACTGGT	
	P	AGTGATAGATCCATTCCTATGACTGT	

362 **Table 1.** List of primers and probes used in the study. F: forward, R: reverse, P: probe.

363 **Immunoprecipitation, western blots, SILAC labeling.** Immunoprecipitations were performed
364 as described with slight modifications.[43] Protein G Dynabeads (Invitrogen) were washed and coated
365 with anti-p55+p24+p17 antibody (Abcam) by rotating for 15 mins at 4°C. After washing off unbound

366 antibody, cleared cell lysates were added to the coated beads and incubated at 4°C with rotation for
367 1 hour. Beads were then separated by a magnet, washed three times and bound proteins were
368 released from the beads by boiling in the presence of a denaturing loading buffer. Released proteins
369 were analyzed by SDS-PAGE and western blot as previously described.[44] Briefly, cells were washed
370 with PBS, scraped, transferred to a tube and washed again with PBS. The pellet was lysed in NP40
371 lysis buffer (100 mM Tris, 30 mM NaCl, 0.5% NP-40) containing benzonase for 15-30 min on ice.
372 Lysates were cleared by centrifugation at 10,000 rpm for 5 min, supplemented with denaturing
373 loading buffer (Invitrogen) and run on an SDS-PAGE. Proteins were transferred to a PVDF membrane
374 (Millipore), blocked by blocking buffer (Rockland) and incubated with primary and IRdye-labeled
375 secondary antibodies (Licor). Blots were visualized on an Odyssey scanner (Licor). Anti-p24 antibody
376 used for HIV-1 capsid detection was AG3.0 (NIH ARP-4121)[45] and 183-H12-5C (NIH-ARP-3537).

377 Labeling and immunoprecipitation for mass spectrometry was performed using the SILAC
378 Protein Quantitation-Trypsin kit and MS-compatible Magnetic IP kit from Pierce (Thermo) according
379 to manufacturer's instructions. Cells were cultured in light medium with 10% dialyzed FBS and
380 transduced with viruses also produced in light medium. The virus used was VSV-G-pseudotyped,
381 NL4.3-Firefly reporter virus carrying 10 amino acids from the p6 region of SIVmac (pNL-luc3-SIVp6[17-
382 26]).[46] Infection was performed in the presence or absence of NVP (25 µM) or CHX (100 µg/ml) at an
383 MOI of 0.5 by spinoculation. The conditions were: Mock (no virus), virus (no drug), virus + NVP, and
384 virus + NVP + CHX. At the time of transduction, cells were switched to heavy medium. After
385 incubation for 18 hours, cells were washed extensively with PBS or PBS+CHX (50 µg/ml) to remove all
386 heavy media and lysed in IP-MS cell lysis buffer with protease inhibitors on ice. Immunoprecipitation
387 was performed with an anti-p24 antibody (183-H12-5C; NIH-ARP-3537) using Pierce Protein A/G
388 magnetic beads. Eluted proteins were analyzed by LC-MS. Samples were prepared and analyzed in
389 biological triplicates.

390 **Liquid chromatography and mass spectrometry.** Peptides were analyzed on an Evosep One
391 liquid chromatography system coupled online via the CaptiveSpray source to a timsTOF HT mass
392 spectrometer (Bruker Daltonics). Peptides were manually loaded onto Evotips Pure (Evosep) and
393 separated using the 30 samples per day (SPD) method on the respective performance column (15 cm
394 x 75 µm, 1.9 µm, Evosep). Column temperature was kept at 40°C using a column toaster (Bruker
395 Daltonics) and peptides were ionized using electrospray with a CaptiveSpray emitter (10 µm i.d.,
396 Bruker Daltonics) at a capillary voltage of 1400 V. The timsTOF HT was operated in ddaPASEF mode in
397 the m/z range of 100-1,700 and in the ion mobility (IM) range of 0.65 – 1.35 Vs cm^{-2}.[47] Singly-charged
398 precursors were filtered out based on their m/z-ion mobility position. Precursor signals above 2,500
399 arbitrary units were selected for fragmentation using a target value of 20,000 arbitrary units and an

400 isolation window width of 2 Th below 700 Da and 3 Th above 700 Da. Afterwards, fragmented
401 precursors were dynamically excluded for 0.4 min. The collision energy was decreased as a function
402 of the IM from 59 eV at 1/K0 = 1.6 Vs cm^{-1} to 20 eV at 1/K0 = 0.6 Vs cm^{-1}. One cycle consisted of 10
403 PASEF ramps.

404 **MS data analysis.** The LC-IMS-MS/MS data were analyzed using FragPipe (version 20.0).[48]
405 Spectra were searched using MSFragger against the protein sequences of the human proteome
406 (UP000005640, UniProtKB) and of HIV-1 (NL4-3 e- r- Fluc [ARP-3418] with a modified SIV p6 between
407 aa 17-26) with a precursor and fragment mass tolerance of 20 ppm, strict trypsin specificity (Lysine:
408 K, Arginine: R) and allowing up to two missed cleavage sites. Cysteine carbamidomethylation was set
409 as a fixed modification and methionine oxidation, N-terminal acetylation of proteins as well as heavy
410 labeling of lysine and arginine (K + 8.014199 Da, R + 10.008269 Da) as variable modifications. Search
411 results were validated using Percolator with MSBooster enabled rescoring and converged to false
412 discovery rates of 1% on all levels. Proteins were quantified using IonQuant based on peptides
413 consistently identified in all replicates and requiring at least 2 peptides per protein.

414 **p24 ELISA.** p24-CA concentrations of viral stocks were determined by a homemade ELISA, as
415 previously described.[45] Briefly, 96-well plates were coated overnight at 4°C with the AG3.0 anti-p24
416 antibody diluted 1:100 in carbonate/bicarbonate buffer (Sigma). The next day, plates were washed
417 three times with wash buffer (PBS+0.05% Tween), blocked with PBS+2% milk powder at 37°C for 1 h
418 and washed again three times. Meanwhile, the viral supernatants were inactivated by incubating
419 with a final concentration of 0.2% Tween for 10 min at room temperature. Serial dilutions of viral
420 supernatants in dilution buffer (PBS+2% milk powder+0.05% Tween) were pipetted into the wells and
421 incubated at 37°C for 1 h. After three washes, the primary antibody in the form of pooled HIV+ serum
422 diluted 1:10000 was added to the wells and incubated at 37°C for 1 h. Following another three
423 washes, the secondary antibody anti-human IgG-HRP (Sigma) was added at 1:1000 dilution. After
424 three more washes, the substrate solution (12.5 ml phosphate/citrate buffer + 1 OPD tablet (5 mg;
425 Sigma) + 12 µl 30% H_2O_2 solution) was added and incubated at room temperature for 10 mins.
426 Reactions were stopped by adding 5% sulphuric acid (H_2SO_4). Absorbance was measured at 492 nm
427 and 620 nm.

428 Statistics

429 All statistics analyses were performed using GraphPad Prism 9. For each figure, the numbers
430 of biological replicates are as follows: Fig. 1B: n=7, Fig. 1C: n=6, Fig. 1D: n=3, Fig. 1E-F: n=2, Fig. 2B:
431 n=3, Fig. 2C: n=7, Fig. 2D-E: n=6, Fig. 2F-G: n=3, Fig. 3A: n=3-6, Fig. 3C-D: n=6, Fig. 3E: n=5, Fig. 3F:
432 n=6-11, Fig. 3G, n=3-6, Fig. 3H, n=6, Fig. 3I-J, n=3, Fig. 4B, n=5, Fig. 4D: n=3, Fig. 4F, n=4, Fig. 5A, n=5-

10, Fig. 5B: n=10, Fig. 5C, n=3, Fig. 5E, n=6, Fig. 5F, n=12. Supp. Fig. 1A: n=2-4, Supp. Fig. 1B-C: n=3, Supp. Fig. 2A: n=2, Supp. Fig. 3A-B, n=3.

Acknowledgements

We thank members of the Cingöz Lab for helpful discussions, Christine Goffinet and her group for valuable input and materials, as well as Igor Minia for help with polysome fractionation. We thank Kornelia Gericke and Sabina Reichert for excellent laboratory management and our colleagues in RKI-FG18. This work was funded by the priority program of the German Research Council (DFG) awarded to OC and NB (SPP1923; innate sensing and restriction of retroviruses), intramural funds from the Robert Koch Institute, as well as the KT Boost Fund awarded to OC by the Klaus Tschira Foundation and the German Scholars Organization (GSO).

Data availability

The data that support the findings of this study are available from the corresponding author upon reasonable request. Large datasets generated in this study have been deposited in the public database PRIDE (https://www.ebi.ac.uk/pride/) under the accession number [N].

448 ## Figures and legends

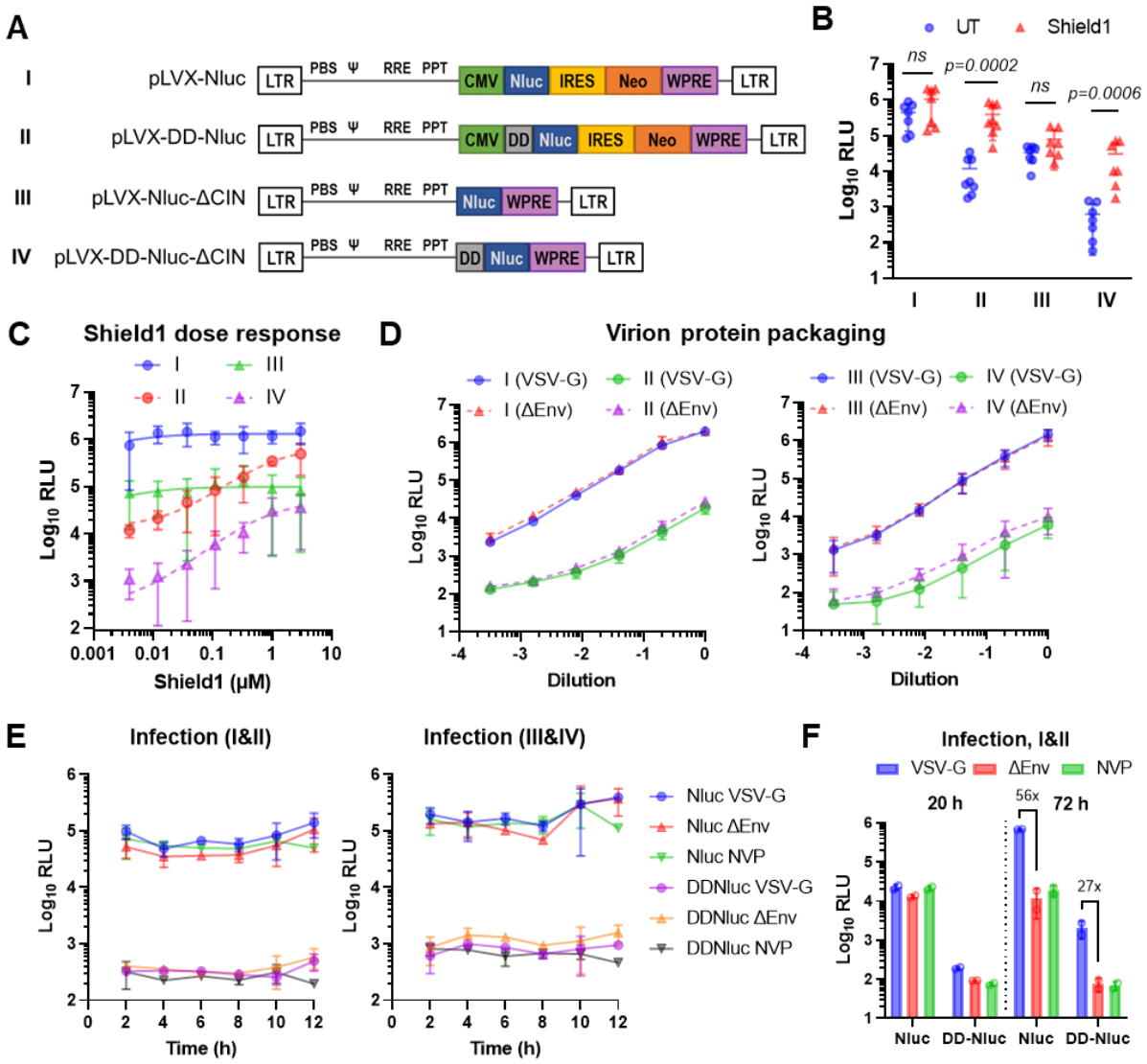

449 ## Figure 1

450 **Figure 1. Posttranslational regulation of protein stability reduces protein packaging into lentiviral particles**
451 **and their delivery into recipient cells.** (A) Schematic representation of the constructs generated, not drawn to
452 scale. Nano-luciferase (Nluc) was inserted with or without a destabilizing domain (DD) downstream of a CMV
453 promoter in a minimal lentiviral vector to generate pLVX-(DD)-Nluc (constructs I & II). The CMV promoter, IRES
454 element and Neomycin resistance gene were deleted to generate pLVX-(DD)-ΔCIN (constructs III & IV). (B) 293T
455 cells were transfected with the indicated constructs in the presence or absence of Shield1. Nluc activity was
456 measured after 24 hours. (C) Transfection was performed as in B using different concentrations of Shield1. (D)
457 Virus supernatants produced using the constructs in A with a packaging plasmid, with or without an Env (VSV-
458 G) were assayed for virion-packaged Nluc activity. (E) Infection was performed with the viruses in D with or
459 without NVP and assayed for Nluc activity at the indicated time points. (F) 293T cells were infected with pLVX-
460 (DD)-Nluc carrying a VSV-G Env in the presence or absence of NVP, or with bald viruses without an Env. Nluc
461 activity was measured at 20 hpi and 72 hpi. IRES: internal ribosomal entry site, WPRE: woodchuck hepatitis
462 virus posttranscriptional regulatory element, PBS: primer binding site, psi (Ψ): packaging signal, RRE: rev-
463 response element, PPT: polypurine tract, NVP: nevirapine. Data are presented as means +/- SD. Statistical
464 analyses were performed by multiple Mann-Whitney tests using the False Discovery Rate (FDR) correction of
465 Benjamini, Krieger and Yekutieli. ns: not significant.

466 **Figure 2**

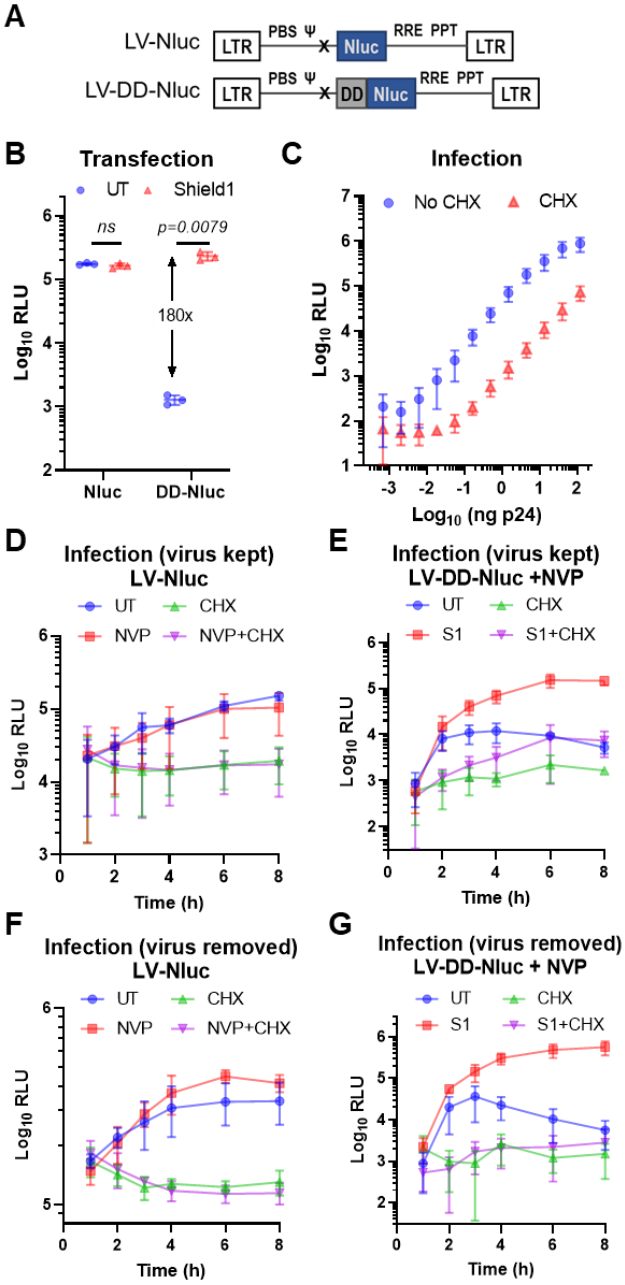

467 **Figure 2. Incoming minimal lentiviral RNA genomes are translated following entry into host cells.**
468 (A) Schematic representation of the lentiviral constructs used; not drawn to scale. Nluc was cloned into a
469 minimal lentiviral vector downstream of the packaging signal (Ψ), with or without the destabilizing domain
470 (DD), and all other heterologous elements (CMV promoter, IRES, Neo resistance gene, WPRE) were removed.
471 (B) Cells were transfected with the constructs in A in the presence or absence of Shield1 (S1). Nluc reporter
472 activity was measured one day later. (C) Cells were infected with serial dilutions of LV-DD-Nluc in the presence
473 of S1 and NVP, with or without cycloheximide (CHX), followed by Nluc measurement. (D,F) Cells were infected
474 with VSV-G pseudotyped LV-Nluc virus in the presence or absence of NVP and/or CHX, where the virus was
475 either kept on the cells (D) or washed away (F). Luciferase activity was measured at the indicated time points.
476 (E,G) Infection was performed as in D and F, but with LV-DD-Nluc and in the presence of NVP, with or without
477 S1 and/or CHX. Data are presented as means +/- SD. Statistical analyses were performed using two-tailed
478 unpaired t-test with Welch's correction. ns: not significant.

479 **Figure 3**

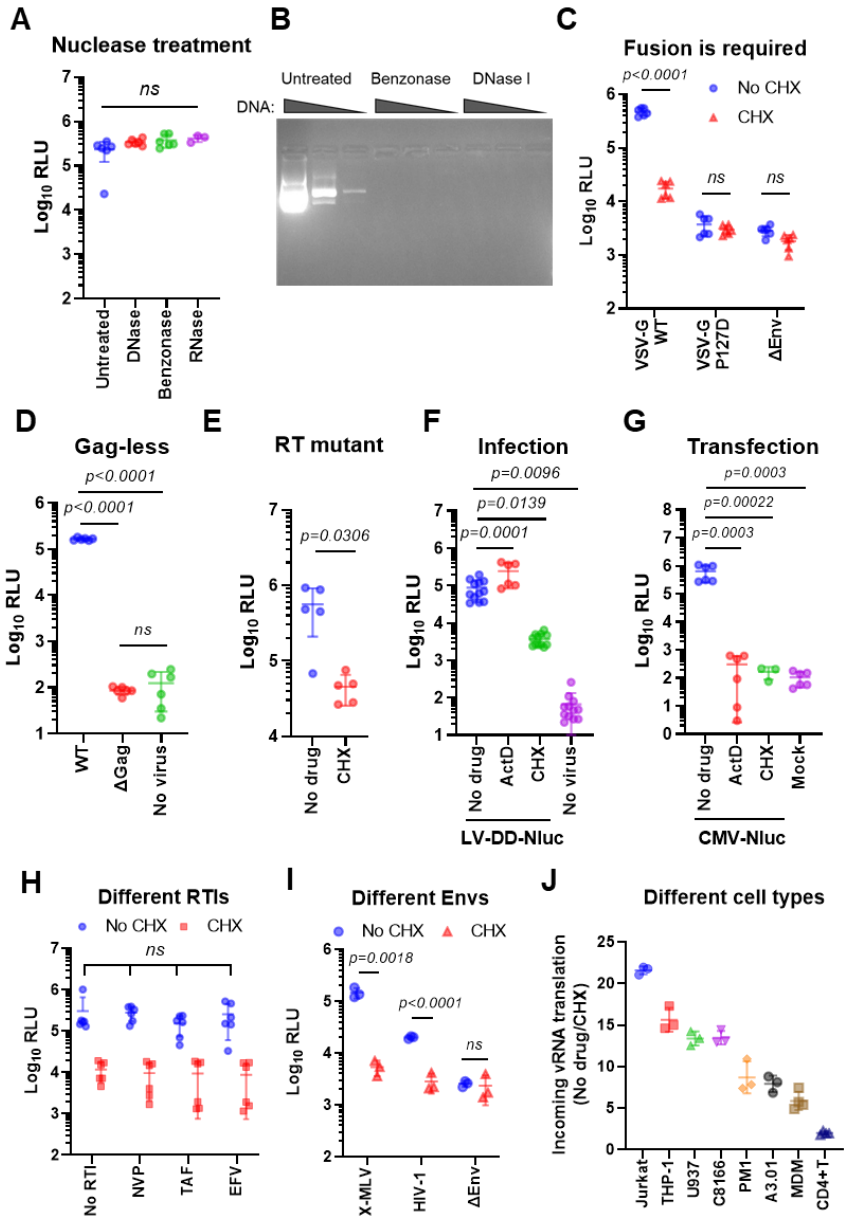

480 **Figure 3. Direct expression from incoming lentiviral RNA genomes is truly due to *de novo* translation and**
481 **independent of reverse transcription.**
482 Unless indicated otherwise, all infections were performed on 293T cells with LV-DD-Nluc virus in the presence
483 of NVP and S1, with or without CHX, and assayed 4-6 hours later. (A) Equal amounts of virus stocks were
484 treated with nucleases or left untreated prior to transduction of cells. (B) Different amounts of plasmid DNA
485 (0.1, 1 or 10 µg) were treated with nucleases or left untreated and visualized on an agarose gel. (C) Cells were
486 transduced with viruses pseudotyped with WT VSV-G, a fusion-deficient mutant of VSV-G (P127D) or without
487 an Env. (D) Transduction with "viruses" produced in the presence or absence of a lentiviral packaging vector
488 (WT vs. ΔGag, respectively). (E) Transduction with reporter virus that carries a catalytic RT mutation (D110E) in
489 the presence of Shield1. (F) Transduction in the presence of S1 and NVP, with or without ActD or CHX. (G)
490 Transfection of cells with a plasmid encoding CMV-driven Nluc in the presence of ActD or CHX. (H) Transduction
491 in the presence of different RT inhibitors at 10 µM. (I) TZM-bl cells were transduced with viruses pseudotyped
492 with HIV-1 Env, X-MLV Env or no Env. (J) The indicated cell types were transduced with reporter viruses.. Data
493 are presented as means +/- SD. Statistical analyses were performed by one-way ANOVA with Tukey's test (A, D,
494 F, G) or by unpaired t-test with Welch's correction (C, E, I). In case of multiple unpaired t-tests, the False
495 Discovery Rate (FDR) correction of Benjamini, Krieger and Yekutieli were used (C, I). ns: not significant. NVP:
496 Nevirapine, EFV: Efavirenz, TDF: Tenofovir Disoproxil Fumarate.

497 **Figure 4**

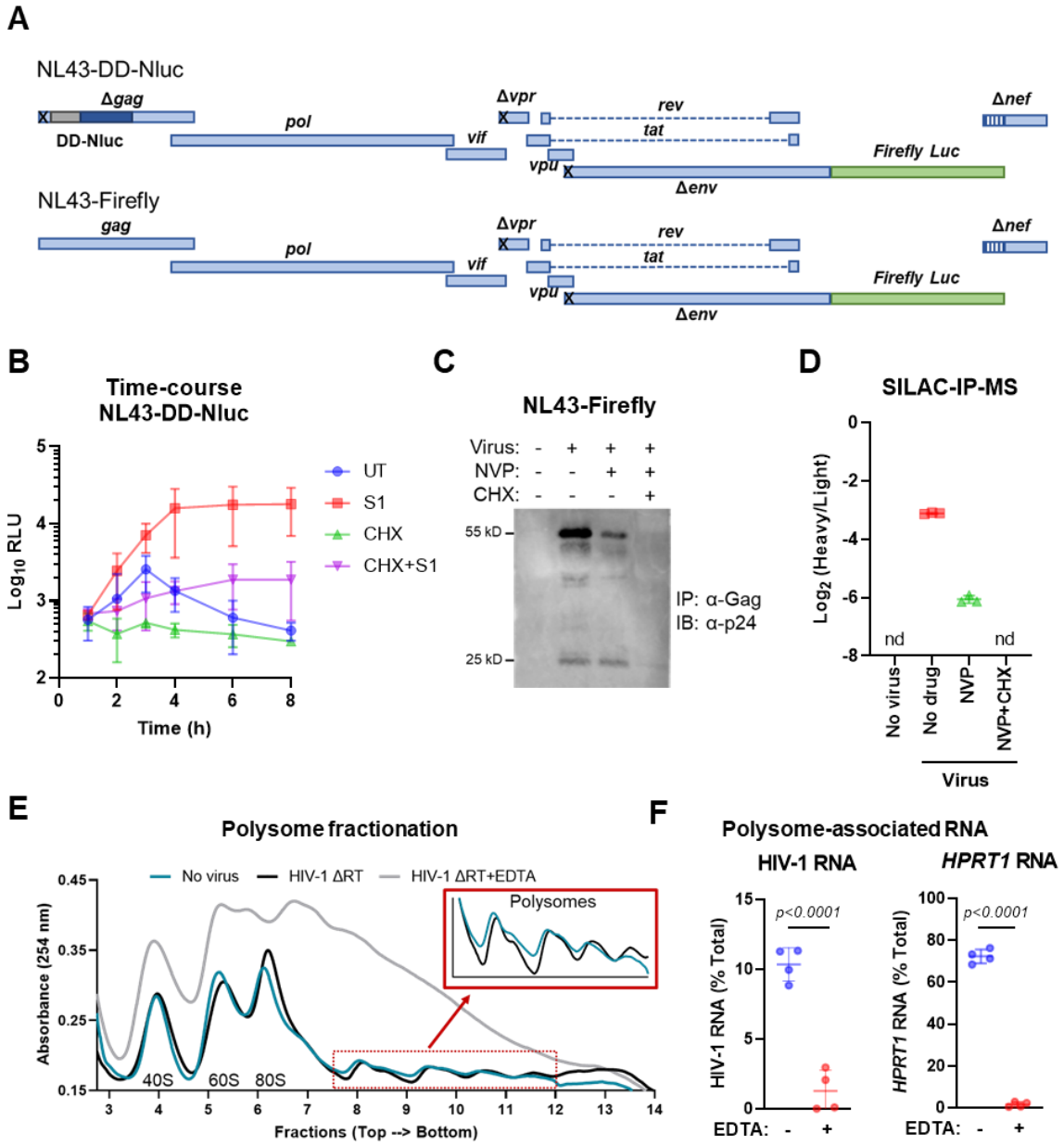

498 **Figure 4. Incoming near full-length HIV-1 genomes are translated to produce viral proteins in the absence of**
499 **reverse transcription.** (A) Schematic representation of the near full-length HIV-1 constructs, where 'x' denotes
500 mutated codons. DD-Nluc was cloned into the NL43-Firefly construct downstream of the packaging signal to
501 generate NL43-DD-Nluc. (B) 293T cells were infected with NL43-DD-Nluc with nevirapine (NVP) in the presence
502 or absence of Shield1 (S1) and/or CHX. Nluc activity was measured at the indicated time points. (C) Cells were
503 infected with VSV-G-pseudotyped NL43-Firefly with or without NVP or CHX. Lysates were collected one day
504 after infection, immunoprecipitated with a polyclonal anti-HIV-1 Gag antibody and probed for p24. (D) Cells
505 were labeled with heavy amino acids (SILAC) at the time of infection (MOI = 0.5) in the presence of the
506 indicated drugs. 18 hours later, Gag was immunoprecipitated from cell lysates and bound proteins were
507 analyzed by mass spectrometry. Data are represented as the heavy to light ratio of peptides that map to Gag.
508 (E) Representative polysome fractionation profiles from 293T cells infected (or not) with VSV-G pseudotyped
509 IIIB ΔRT (with a catalytic RT mutation DD185/186AA) at 4 hpi and lysed in the presence or absence of EDTA.
510 Lysates were run on a sucrose density gradient, then fractions were collected from top to bottom while
511 simultaneously measuring UV absorbance. (F) RNA was isolated from each fraction and the levels of HIV-1
512 genomic RNA and *HPRT1* were measured by RT-qPCR. The amount of each RNA is given as a percentage of total
513 RNA for that message. Data represent mean +/- SD. Statistical significance was determined by unpaired t-test
514 with Welch's correction, nd: not detected.

515 **Figure 5**

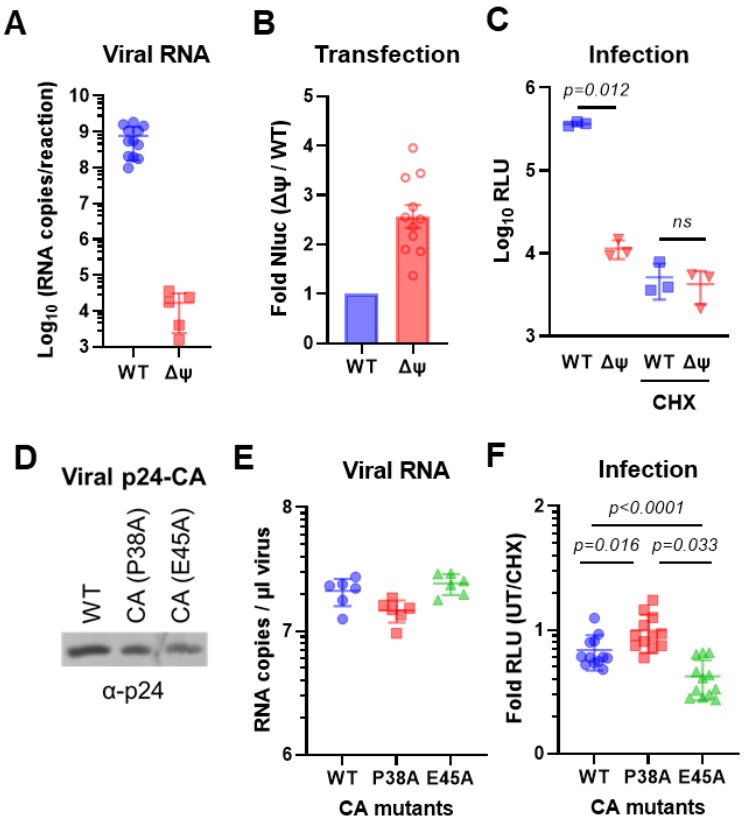

516 **Figure 5. Packaging signal and capsid stability affect the translation of incoming RNA genomes.**
517 (A) Viral RNA content of LV-DD-Nluc viruses produced with or without a deletion between nucleotides 750-787
518 in the packaging signal (ΔΨ; delta psi) measured by RT-qPCR. (B) 293T cells were transfected with the LV-DD-
519 Nluc WT or ΔΨ construct and subjected to luciferase assay one day later. (C) Cells were transduced with WT or
520 ΔΨ viruses; expression from the incoming viral genome was analyzed by luciferase assay at 4-6 hpi. (D) Western
521 blot of p24-CA in concentrated WT or the indicated capsid mutant virus stocks. (E) RT-qPCR for quantification of
522 viral RNA. (F) Cells were transduced with reporter viruses carrying WT or mutated CA. All transductions were
523 performed in 293T cells using LV-DD-Nluc viruses in the presence of both NVP and Shield1, with or without
524 CHX. Data represent mean +/- SD. Statistical significance was determined by unpaired t-test with Welch's
525 correction (C) or one-way ANOVA with Tukey's correction (F). ns: not significant.

526 **Supplementary Figures and Legends**

527 **Supp. Figure 1**

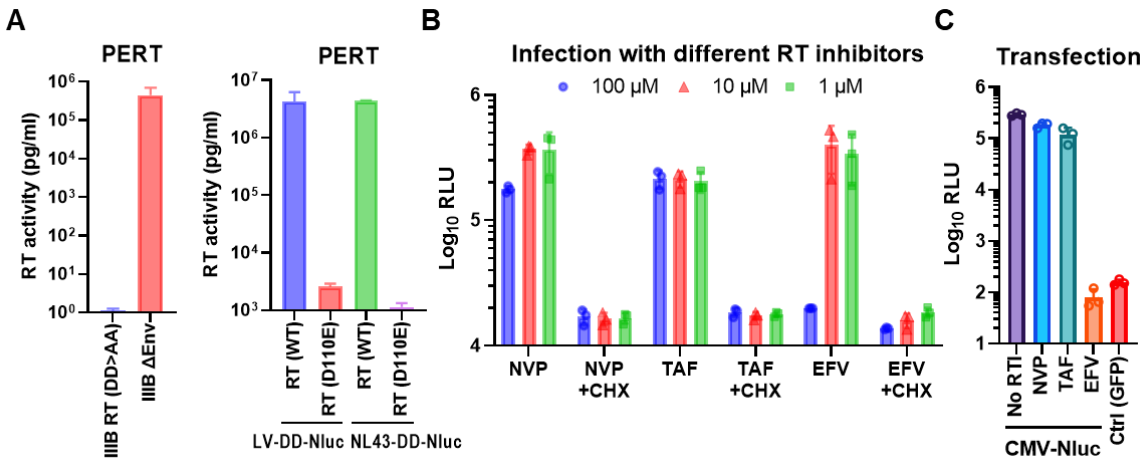

528 **Supplementary Figure 1. Loss of RT activity by catalytic mutations or the use of different RT inhibitors.**
529 (A) PERT assay on RT catalytic mutant virus HIV-1 IIIB (DD185/186AA) used in polysome fractionation, or the LV-
530 DD-Nluc and NL43-DD-Nluc viruses produced with the RT catalytic mutant packaging vector (D110E) used in
531 reporter assays. (B) Luciferase assay on cells transduced with LV-DD-Nluc virus in the presence of 1-100 µM of
532 the RT inhibitors, with or without CHX. (C) Cells were transfected with a CMV-driven Nluc construct in the
533 presence of 100 µM RT inhibitors. Toxicity was measured by luciferase assay 6 hours after transfection. NVP:
534 Nevirapine, EFV: Efavirenz, TDF: Tenofovir disoproxil fumarate. Data represent mean +/- SD.
535

536 **Supp. Figure 2**

537

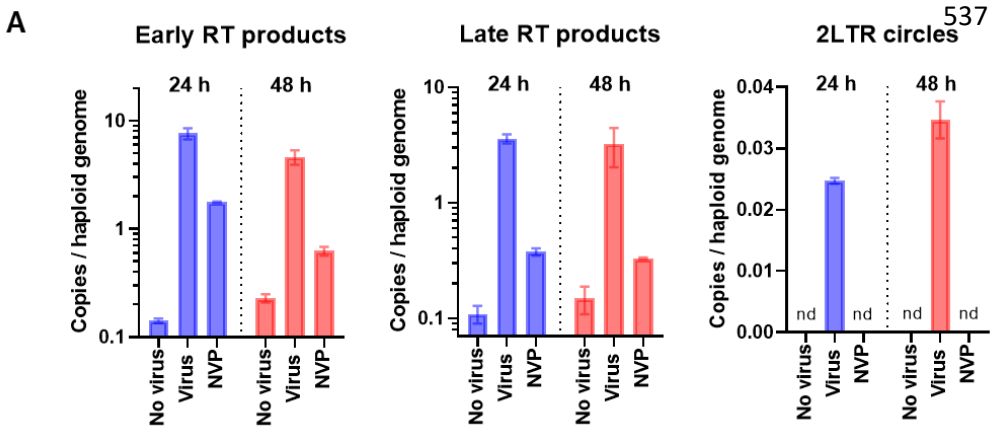

538 **Supplementary Figure 2. Quantification of post-entry events after virus challenge.**
539 (A) 293T cells were infected with NL43-Firefly virus (40 ng/100K cells) and DNA was isolated at 24 and 48 hours
540 post-infection. Early and late RT products, as well as 2-LTR circles were quantified by qPCR.

541 **Supp. Figure 3**

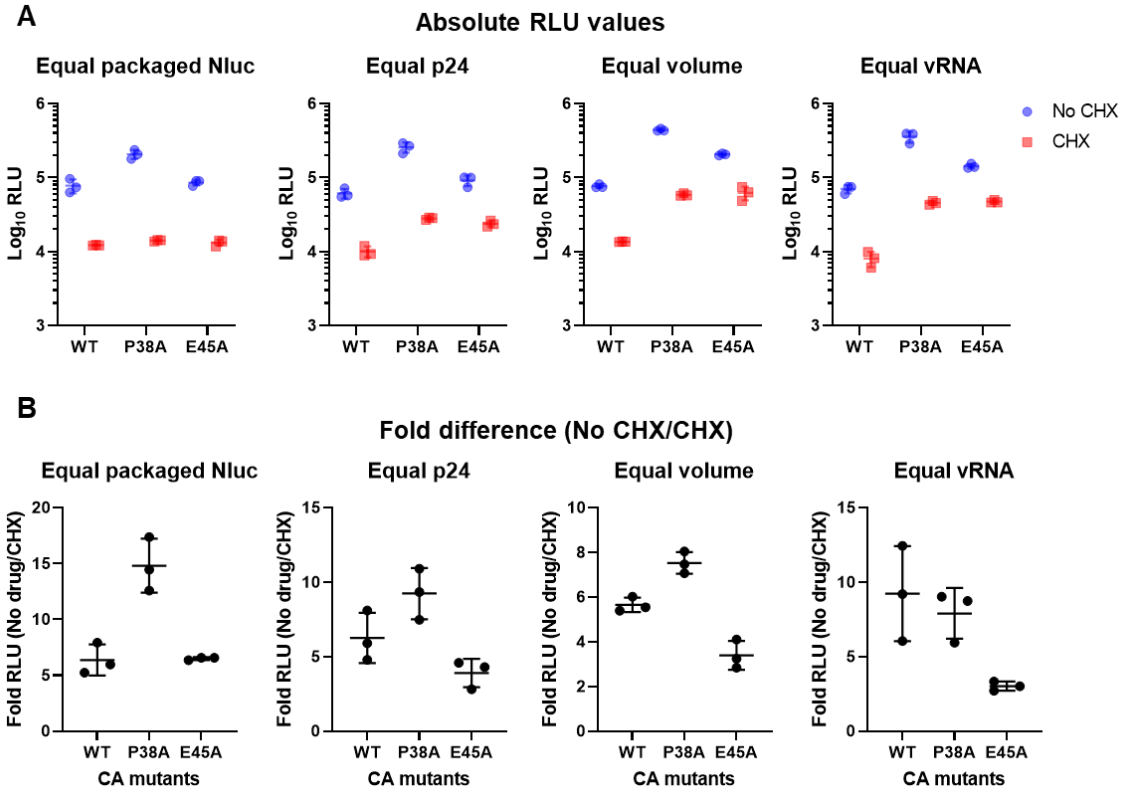

542 **Supplementary Figure 3. Capsid stability mutations alter the translation potential of incoming retroviral**
543 **genomes.**
544 (A) Cells were infected with LV-DD-Nluc viruses containing WT, P38A or E45A capsids in the presence of NVP
545 and Shield1, with or without CHX. Virus stocks were normalized based on either p24, viral RNA, virion-packaged
546 Nluc or simple volume. (B) Fold difference between CHX-treated and untreated samples based on the data in
547 (A). Data represent mean +/- SD.

548 # References

549 1. Brown JD*, et al.* Structural basis for transcriptional start site control of HIV-1 RNA fate. *Science (New York, NY)* **368**,
550 413-417 (2020).
551 2. Kharytonchyk S*, et al.* Transcriptional start site heterogeneity modulates the structure and function of the HIV-1
552 genome. *PNAS* **113**, 13378-13383 (2016).
553 3. Rawson JMO, Nikolaitchik OA, Shakya S, Keele BF, Pathak VK, Hu WS. Transcription Start Site Heterogeneity and
554 Preferential Packaging of Specific Full-Length RNA Species Are Conserved Features of Primate Lentiviruses. *Microbiol*
555 *Spectr* **10**, e0105322 (2022).
556 4. Singh G, Seufzer B, Song Z, Zucko D, Heng X, Boris-Lawrie K. HIV-1 hypermethylated guanosine cap licenses
557 specialized translation unaffected by mTOR. *PNAS* **119**, e2105153118 (2022).
558 5. Ghysdael J, Kettmann R, Burny A. Translation of bovine leukemia virus virion RNAs in heterologous protein-
559 synthesizing systems. *Journal of virology* **29**, 1087-1098 (1979).
560 6. Kobayashi N, Yamamoto N, Koyanagi Y, Schneider J, Hunsmann G, Hatanaka M. Translation of HTLV (human T-cell
561 leukemia virus) RNA in a nuclease-treated rabbit reticulocyte system. *Embo j* **3**, 321-325 (1984).
562 7. Philipson L, Andersson P, Olshevsky U, Weinberg R, Baltimore D, Gesteland R. Translation of MuLV and MSV RNAs in
563 nuclease-treated reticulocyte extracts: Enhancement of the gag-pol polypeptide with yeast suppressor tRNA. *Cell*
564 **13**, 189-199 (1978).
565 8. Nash KL, Lever AM. Green fluorescent protein: green cells do not always indicate gene expression. *Gene therapy* **11**,
566 882-883 (2004).
567 9. Liu ML, Winther BL, Kay MA. Pseudotransduction of hepatocytes by using concentrated pseudotyped vesicular
568 stomatitis virus G glycoprotein (VSV-G)-Moloney murine leukemia virus-derived retrovirus vectors: comparison of
569 VSV-G and amphotropic vectors for hepatic gene transfer. *Journal of virology* **70**, 2497-2502 (1996).
570 10. Geering B, Schmidt-Mende J, Federzoni E, Stoeckle C, Simon HU. Protein overexpression following lentiviral infection
571 of primary mature neutrophils is due to pseudotransduction. *Journal of immunological methods* **373**, 209-218
572 (2011).
573 11. Gallardo HF, Tan C, Ory D, Sadelain M. Recombinant retroviruses pseudotyped with the vesicular stomatitis virus G
574 glycoprotein mediate both stable gene transfer and pseudotransduction in human peripheral blood lymphocytes.
575 *Blood* **90**, 952-957 (1997).
576 12. Kim JT*, et al.* Dendritic cell-targeted lentiviral vector immunization uses pseudotransduction and DNA-mediated
577 STING and cGAS activation. *Sci Immunol* **2**, eaal1329 (2017).
578 13. Haas DL, Case SS, Crooks GM, Kohn DB. Critical Factors Influencing Stable Transduction of Human CD34+ Cells with
579 HIV-1-Derived Lentiviral Vectors. *Molecular Therapy* **2**, 71-80 (2000).
580 14. Banaszynski LA, Chen L-c, Maynard-Smith LA, Ooi AGL, Wandless TJ. A Rapid, Reversible, and Tunable Method to
581 Regulate Protein Function in Living Cells Using Synthetic Small Molecules. *Cell* **126**, 995-1004 (2006).
582 15. England CG, Ehlerding EB, Cai W. NanoLuc: A Small Luciferase Is Brightening Up the Field of Bioluminescence.
583 *Bioconjugate Chemistry* **27**, 1175-1187 (2016).
584 16. Donahue DA, Sloan RD, Kuhl BD, Bar-Magen T, Schader SM, Wainberg MA. Stage-dependent inhibition of HIV-1
585 replication by antiretroviral drugs in cell culture. *Antimicrob Agents Chemother* **54**, 1047-1054 (2010).
586 17. Murray JM, Kelleher AD, Cooper DA. Timing of the components of the HIV life cycle in productively infected CD4+ T
587 cells in a population of HIV-infected individuals. *Journal of virology* **85**, 10798-10805 (2011).
588 18. Watts JM*, et al.* Architecture and secondary structure of an entire HIV-1 RNA genome. *Nature* **460**, 711-716 (2009).
589 19. Rein A. RNA Packaging in HIV. *Trends in Microbiology* **27**, 715-723 (2019).
590 20. Geraerts M, Willems S, Baekelandt V, Debyser Z, Gijsbers R. Comparison of lentiviral vector titration methods. *BMC*
591 *Biotechnology* **6**, 34 (2006).
592 21. Gallis BM, Eisenman RN, Diggelmann H. Synthesis of the precursor to avian RNA tumor virus internal structural
593 proteins early after infection. *Virology* **74**, 302-313 (1976).
594 22. Shurtz R, Dolev S, Aboud M, Salzberg S. Viral genome RNA serves as messenger early in the infectious cycle of
595 murine leukemia virus. *Journal of virology* **31**, 668-676 (1979).
596 23. Tobaly J, d'Auriol L, Yang WK, Peries J, Emanoil-Ravicovitch R. Murine retrovirus genome directs the synthesis of gag
597 protein precursor early after infection. *Biochimie* **64**, 969-973 (1982).
598 24. Caliskan N KA, Buck S, Gribling A-S, Gilmer O, Pekarek L, Bohn P, Koch T, Mireisz CN-M, Schlosser A, Erhard F, Smyth
599 R. The translational landscape of HIV-1 infected cells reveals novel gene regulatory principles. Preprint at
600 https://www.researchsquare.com/article/rs-3352709/v3352701 (2023).
601 25. Labaronne E*, et al.* Extensive uORF translation from HIV-1 transcripts conditions DDX3 dependency for expression of
602 main ORFs and elicits specific T cell immune responses in infected individuals. Preprint at
603 https://www.biorxiv.org/content/10.1101/2022.1104.1129.489990v489991.full (2022).
604 26. Baum C, Schambach A, Bohne J, Galla M. Retrovirus Vectors: Toward the Plentivirus? *Molecular Therapy* **13**, 1050-
605 1063 (2006).
606 27. Galla M, Will E, Kraunus J, Chen L, Baum C. Retroviral pseudotransduction for targeted cell manipulation. *Molecular*
607 *cell* **16**, 309-315 (2004).

608 28. Mock U*, et al.* Novel lentiviral vectors with mutated reverse transcriptase for mRNA delivery of TALE nucleases.
609 *Scientific Reports* **4**, 6409 (2014).
610 29. Counsell JR*, et al.* Re-structuring lentiviral vectors to express genomic RNA via cap-dependent translation. *Molecular*
611 *Therapy* **20**, 357-365 (2021).
612 30. Zila V*, et al.* Cone-shaped HIV-1 capsids are transported through intact nuclear pores. *Cell* **184**, 1032-1046.e1018
613 (2021).
614 31. Burdick RC*, et al.* HIV-1 uncoats in the nucleus near sites of integration. *Proceedings of the National Academy of*
615 *Sciences* **117**, 5486-5493 (2020).
616 32. Müller TG*, et al.* HIV-1 uncoating by release of viral cDNA from capsid-like structures in the nucleus of infected cells.
617 *eLife* **10**, e64776 (2021).
618 33. Li C, Burdick RC, Nagashima K, Hu WS, Pathak VK. HIV-1 cores retain their integrity until minutes before uncoating in
619 the nucleus. *Proceedings of the National Academy of Sciences of the United States of America* **118**, (2021).
620 34. Klasse PJ. Molecular determinants of the ratio of inert to infectious virus particles. *Prog Mol Biol Transl Sci* **129**, 285-
621 326 (2015).
622 35. Da Silva Santos C, Tartour K, Cimarelli A. A Novel Entry/Uncoating Assay Reveals the Presence of at Least Two
623 Species of Viral Capsids During Synchronized HIV-1 Infection. *PLOS Pathogens* **12**, e1005897 (2016).
624 36. Sacha JB*, et al.* Gag-specific CD8+ T lymphocytes recognize infected cells before AIDS-virus integration and viral
625 protein expression. *J Immunol* **178**, 2746-2754 (2007).
626 37. Sacha JB*, et al.* Pol-specific CD8+ T cells recognize simian immunodeficiency virus-infected cells prior to Nef-
627 mediated major histocompatibility complex class I downregulation. *J Virol* **81**, 11703-11712 (2007).
628 38. Bauby H*, et al.* HIV-1 Vpr Induces Widespread Transcriptomic Changes in CD4⁺ T Cells Early
629 Postinfection. *mBio* **12**, e01369-01321 (2021).
630 39. Hong S*, et al.* Fibrils of prostatic acid phosphatase fragments boost infections with XMRV (xenotropic murine
631 leukemia virus-related virus), a human retrovirus associated with prostate cancer. *Journal of virology* **83**, 6995-7003
632 (2009).
633 40. Cingöz O, Goff SP. Cyclin-dependent kinase activity is required for type I interferon production. *PNAS* **115**, E2950-
634 e2959 (2018).
635 41. Mbisa JL, Delviks-Frankenberry KA, Thomas JA, Gorelick RJ, Pathak VK. Real-time PCR analysis of HIV-1 replication
636 post-entry events. *Methods Mol Biol* **485**, 55-72 (2009).
637 42. Malnati MS*, et al.* A universal real-time PCR assay for the quantification of group-M HIV-1 proviral load. *Nature*
638 *Protocols* **3**, 1240-1248 (2008).
639 43. Zhu Y, Wang GZ, Cingöz O, Goff SP. NP220 mediates silencing of unintegrated retroviral DNA. *Nature* **564**, 278-282
640 (2018).
641 44. Cingöz O, Arnow ND, Puig Torrents M, Bannert N. Vpx enhances innate immune responses independently of
642 SAMHD1 during HIV-1 infection. *Retrovirology* **18**, 4 (2021).
643 45. Sanders-Beer BE, Eschricht M, Seifried J, Hirsch VM, Allan JS, Norley S. Characterization of a monoclonal anti-capsid
644 antibody that cross-reacts with three major primate lentivirus lineages. *Virology* **422**, 402-412 (2012).
645 46. Sunseri N, O'Brien M, Bhardwaj N, Landau NR. Human Immunodeficiency Virus Type 1 Modified To Package Simian
646 Immunodeficiency Virus Vpx Efficiently Infects Macrophages and Dendritic Cells. *Journal of virology* **85**, 6263-6274
647 (2011).
648 47. Meier F*, et al.* Online Parallel Accumulation-Serial Fragmentation (PASEF) with a Novel Trapped Ion Mobility Mass
649 Spectrometer. *Mol Cell Proteomics* **17**, 2534-2545 (2018).
650 48. Yu F, Haynes SE, Teo GC, Avtonomov DM, Polasky DA, Nesvizhskii AI. Fast Quantitative Analysis of timsTOF PASEF
651 Data with MSFragger and IonQuant. *Mol Cell Proteomics* **19**, 1575-1585 (2020).